Int. J. Solids Structures Vol. 24, No. 5, pp. 481–496, 1988
Printed in Great Britain.

0020-7683/88 $3.00 + .00

A VERSATILE MODEL FOR INTERACTIVE BUCKLING OF COLUMNS AND BEAM-COLUMNS

M. ASHRAF ALI† and SRINIVASAN SRIDHARAN
Department of Civil Engineering, Washington University, St. Louis, MO 63130, U.S.A.

(*Received* 16 *May* 1987; *in revised form* 30 *September* 1987)

Abstract—A new formulation has been developed to study the interactive buckling of thin-walled columns having arbitrary cross-sections. The emphasis in this paper is, however, on columns with a single axis of symmetry. The formulation is designed to take into account the simultaneous interaction of the purely flexural and flexural–torsional overall modes of buckling with local buckling. The local buckling deformations are described in terms of a primary local mode together with two secondary local modes of the same wavelength. The latter are triggered by the interaction of bending in two perpendicular planes with the primary local mode. The three eigenmodes and the six second-order in-plane displacement fields are all computed using a finite-strip technique. The modulation of the amplitudes of the local modes and the overall displacements are described in terms of a one-dimensional finite element model. Thus a new beam element which has embedded in it the local buckling information is developed. It appears that the present analytical model is very versatile being applicable to members of arbitrary cross-section and end conditions. For columns with a single axis of symmetry, it is seen that there exists a non-linear coupling between the purely flexural and the flexural–torsional modes of buckling via local buckling deformation. Typical examples of channel section columns are presented. It is shown that the channel section columns of commonly used proportions are highly imperfection sensitive in the context of combined interaction of the enumerated modes of buckling. This sensitivity remains even for columns with well separated overall and local critical stresses—a feature which is in stark contrast with the behavior of the Tvergaard panel.

NOTATION

$[D]$	constitutive relationship matrix
E	Young's modulus
L	length of the member
L_e	length of a beam element
M_x, M_y, M_{xy}	bending moments in the x–z and y–z planes and twisting moment
N_x, N_y, N_{xy}	in-plane force resultants, normal in x- and y-directions and shear
U	axial displacement at the centroid due to overall action
V, W	lateral displacements in the Y- and Z-directions of the shear center
$\bar{V}, \bar{W}$	initial imperfection amplitudes in the Y- and Z-directions
X, Y, Z	global coordinates for the description of overall action
c	perimeter of the section
m	number of half-waves of buckling
t	thickness of plate element
t_s	thickness of stiffener
u_1, v_1, w_1	displacement components in the x-, y- and z-directions due to local buckling
x, y, z	local coordinate system used to define local buckling deformation
$\bar{x}$	$2x/L_e$
y_0	The distance between shear center and centroid for a section with an axis of symmetry
$\varepsilon_x, \varepsilon_y, \gamma_{xy}$	in-plane strain components, normal in the x- and y-directions and shear
$\theta, \bar{\theta}$	angle of twist and the initial imperfection in the form of twist at the center of the column
ν	Poisson's ratio
ξ_i	scaling factors for the local buckling modes (mid-span amplitudes)
$\bar{\xi}_i$	initial imperfection amplitudes (maximum values across the section) divided by t
σ	average axial stress carried by any section
σ_i	local critical stress in the ith mode
σ_u	maximum of σ carried by the member
$\chi_x, \chi_y, \chi_{xy}$	curvatures in the x–z and y–z planes and the twist.

INTRODUCTION

The interaction of local and overall buckling in columns has been the subject of intense study by several investigators[1–5]. The imperfection sensitivity of thin-walled columns and the drastic reduction in the load carrying capacity of long columns caused by local buckling

† Present address: Illinois Department of Transportation, Springfield, IL 62704, U.S.A.

are the reasons why interactive buckling has received so much attention. The method of analysis generally consists of the following steps.

(i) Determine by separate analyses the respective eigen-modes and the second-order fields together with the mixed second-order field which arises by the interaction.

(ii) Pose the problem as one of two degrees of freedom, namely the scaling factors of the eigen-modes ξ_i ($i = 1, 2$) using the theory of mode interaction[5]. Since the displacement fields are known in terms of ξ_i, it is possible to write a potential energy function in terms of ξ_i. This procedure works satisfactorily[1, 2] as long as no additional modes are triggered by the interaction.

In the case of doubly symmetric sections the interaction of overall bending with the local buckling mode associated with the smallest critical stress σ_1 (primary local mode) triggers a secondary local mode of the same wavelength. This phenomenon was discussed by the authors in an earlier paper[6]. When this happens, the accuracy of two-mode analysis is open to question in cases for which the two local critical stresses are close to each other. This difficulty was removed by incorporating the secondary local mode liable to be triggered in the interaction as one of the participating modes in the analysis. The resulting three-mode interaction analysis for thin-walled columns is described in Ref. [6].

The interaction of overall bending with local buckling has yet another important feature which is sometimes overlooked. This is the "amplitude modulation", the slow variation of the amplitudes of local buckling along the length of the column[1, 2]. A simple explanation of how this phenomenon arises is available in Ref. [7]. In Ref. [7], the authors employed a finite element description for both the amplitude modulation and the overall bending behavior. This development makes it possible to investigate with ease, columns and beam-columns with end conditions other than simply supported. However, the treatment was restricted to members with doubly symmetric cross-sections.

In this paper, a new comprehensive formulation capable of handling columns and beam-columns of arbitrary cross-section subject to interactive buckling is described. Simultaneous interaction of up to three relevant local modes with overall modes which may be flexural and/or flexural–torsional in character is within the purview of the new model. A new beam element is introduced which has in it embedded all the relevant local buckling information and has the degrees of freedom to depict biaxial bending, twisting and amplitude modulation.

It is well known that columns having open sections are susceptible to buckle in flexural–torsional modes. A thin-walled column with an open section with a single axis of symmetry has a mode of buckling in which bending at right angles to the line of symmetry and twisting are coupled. If this mode is activated, the symmetry of local buckling tends to be lost as a result of the additional compression thrown on one side of the axis of symmetry. [This happens due to a triggering of a secondary mode, which is illustrated for a channel section column in Fig. 3(c).] Thus, there occurs an unsymmetric distribution of the effective stiffness across the section and, as a result, there occurs a coupling of the flexural–torsional mode with the (otherwise uncoupled) flexural buckling in the plane of symmetry. Even in the case of a section for which the flexural buckling in the plane of symmetry is the governing critical mode, such a coupling may occur as a result of initial imperfections or lateral loads perpendicular to the line of symmetry, which destroy the symmetry of local buckling deformation. Again, as already mentioned, bending in each plane will trigger a secondary mode—an effect which is important for sections undergoing significant local buckling deformation on either side of the axes of bending. Thus, for an interactive buckling analysis to be general, the analytical model must incorporate two secondary local modes in addition to the primary one, as well as biaxial bending and twisting of the member (Fig. 3). This is precisely the scope of the present model. As in the earlier works of the authors, the local buckling and the post-local (second-order) fields are obtained using finite strips and, these fields are duly embedded in a beam element capable of biaxial bending and twisting. For simplicity, attention in this paper is restricted to columns having a single axis of symmetry. In what follows, the theory is briefly outlined, and some typical examples of channel-section columns and stiffened panels are considered.

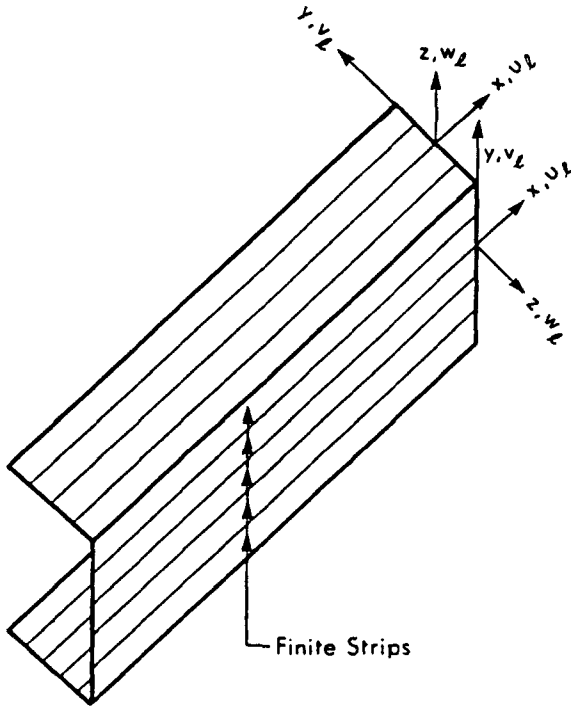

Fig. 1. Local coordinate system of plate elements and finite strip configuration for the description of the local buckling deformation.

THEORY

The local buckling problem

The displacement components due to local buckling at any point on the middle surface of a member of a plate structure (Fig. 1) are given by[7]

$$\begin{Bmatrix} u_l \\ v_l \\ w_l \end{Bmatrix} = \begin{Bmatrix} 0 \\ 0 \\ w_i \end{Bmatrix} \xi_i + \begin{Bmatrix} u_{ij} \\ v_{ij} \\ 0 \end{Bmatrix} \xi_i \xi_j \tag{1}$$

where ξ_i are the scaling factors of the local modes; subscript "l" refers to local buckling; w_i are the appropriately normalized local buckling modes, given by[8–10]

$$w_i = \bar{w}_i(y) \sin\left(\frac{m\pi x}{L}\right) \tag{2}$$

in which $\bar{w}_i(y)$ describes the shape of the ith mode across the section, m is the number of half-waves of local buckling and L the length of the structure. The second-order in-plane displacement field associated with the ith mode is given by u_{ij}, v_{ij} $(i = j)$. The mixed second-order field arising from the interaction of the ith and the jth local modes is given by u_{ij}, v_{ij} $(i \neq j)$, respectively. For any given end-shortening, these displacements take the form[8–10]

$$u_{ij} = \bar{u}_{ij}(y) \sin(2m\pi x/L) \tag{3a}$$

$$v_{ij} = \bar{v}_{ij,0}(y) + \bar{v}_{ij,0}(y) \cos(2m\pi x/L). \tag{3b}$$

All the functions of y in eqns (2) and (3) are easily determined using the finite strip method[10]. Thus the local buckling displacements are known in terms of ξ_i. These are considered as "slowly varying" in the subsequent analysis.

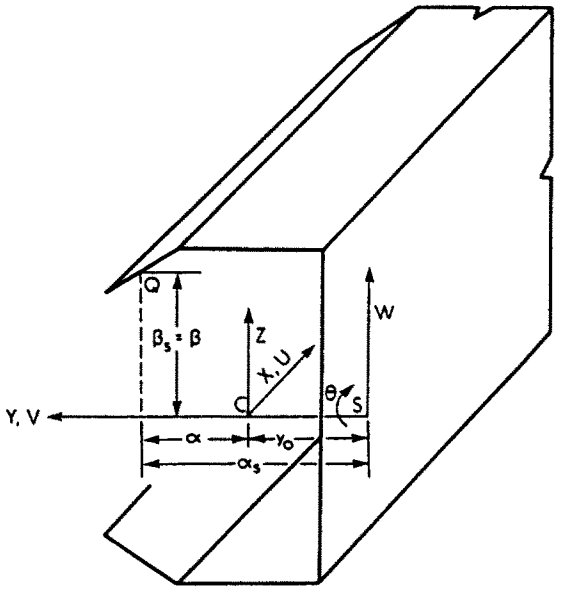

Fig. 2. Global coordinate system for the description of overall buckling deformation: C, centroid; S, shear center.

Overall displacement

The overall behavior is modelled by the usual assumptions of the beam theory. Thus, the shear deformation associated with variable overall bending and the intrinsic and/or external restraints to warping of the cross-section, as well as the normal stress in the transverse direction, are neglected. The displacements of the entire section are then conveniently expressed in terms of U, the axial displacement at the centroid, the lateral displacements of the shear center (V and W, respectively, parallel and perpendicular to the line of symmetry), and the angle of twist θ of the section about the shear center. The quantities U, V, W, and θ are functions of x only.

Figure 2 illustrates the motion of a point Q on the center line of a plate element of a column with a single axis of symmetry. The centroid C is the origin of the coordinate system; the principal axes of the section are the reference axes in the plane of the section. The displacements of the shear center S along the Y-axis (the axis of symmetry) and the Z-axis are V and W, respectively. The overall displacements of $Q(V^0, W^0)$ in the transverse plane are related to the corresponding displacements of S as follows:

$$V^0 = V - \beta_s(y)\theta \tag{4a}$$

$$W^0 = W + \alpha_s(y)\theta \tag{4b}$$

where α_s and β_s are the distances measured along the Y- and Z-axes, respectively, from Q to S.

The contribution to the axial displacement at Q, U^0, of the overall action is given by[11]

$$U^0 = U - \left[\alpha(y)\frac{dV}{dx} + \beta(y)\frac{dW}{dx} + \frac{d\theta}{dx}\{\bar{\omega} - \omega(y)\}\right] \tag{5}$$

where ω is the warping function given by

$$\omega(y) = \int_0^y \rho(s)\, ds \tag{6}$$

in which ρ defines the perpendicular distance from the shear center to the tangent to the profile at any point distant y from a free edge of the profile measured along the profile.

In eqn (5) $\bar{\omega}$ is the averaged value of ω, i.e.

$$\bar{\omega} = \frac{1}{c}\int_0^c \omega(s)\, \mathrm{d}s \tag{7}$$

where c is the perimeter of the profile; α and β are the distances of Q from the centroid along the Y- and Z-axes, respectively.

The strain–displacement relations

The components of the middle surface strain (ε_x, ε_y, and γ_{xy}) and curvature (χ_x, χ_y, χ_{xy}) of the plate elements $\{\varepsilon\}$ are related to the displacements as follows:

$$\varepsilon_x = \left[\frac{\partial u_1}{\partial x} + \frac{1}{2}\left(\frac{\partial w_1}{\partial x}\right)^2\right] + \left[\frac{\partial U^0}{\partial x} + \frac{1}{2}\left\{\left(\frac{\partial V^0}{\partial x}\right)^2 + \left(\frac{\partial W^0}{\partial x}\right)^2\right\}\right]$$

$$\varepsilon_y = \left[\frac{\partial v_1}{\partial y} + \frac{1}{2}\left(\frac{\partial w_1}{\partial y}\right)^2\right] - \nu\left[\frac{\partial U^0}{\partial x} + \frac{1}{2}\left\{\left(\frac{\partial V^0}{\partial x}\right)^2 + \left(\frac{\partial W^0}{\partial x}\right)^2\right\}\right]$$

$$\gamma_{xy} = \frac{\partial v_1}{\partial x} + \frac{\partial u_1}{\partial y} + \left(\frac{\partial w_1}{\partial x}\right)\left(\frac{\partial w_1}{\partial y}\right)$$

$$\chi_x = \frac{\partial^2 w_1}{\partial x^2}; \quad \chi_y = \frac{\partial^2 w_1}{\partial y^2}; \quad \chi_{xy} = 2\left(\frac{\partial^2 w_1}{\partial x\, \partial y} + 2\frac{\mathrm{d}\theta}{\mathrm{d}x}\right). \tag{8a–f}$$

In the foregoing relations, the axial strain ε_x consists of two parts, one a contribution of local buckling and the other of overall action. Notably, the bilinear interaction term involving the overall displacement component normal to the plate element and w_1 has been neglected. This term is of an order of magnitude smaller than the corresponding quadratic term consisting of w_1 only, in so far as the overall bending slope is a slowly varying function compared to the local one; once this term is neglected, it follows that the interaction of overall and local buckling modes can generate only a modification of the local normal displacement field and the in-plane displacements of the corresponding mixed second-order field vanish—a postulate in this and earlier studies on interactive buckling[6, 7]. Thus, neglecting the said bilinear term is not only justified by its smallness, but also warranted from the point of view of consistency. (However, it is necessary to retain both the linear and quadratic terms in the overall displacements in order for the overall buckling to occur and remain inextensional.) The in-plane strain term ε_y involves a Poisson's contribution associated with ε_x in order to eliminate the normal stresses in the transverse direction caused by overall buckling. Note that the twist term χ_{xy} consists of two terms inside the parentheses. The first term is the familiar twist associated with local plate buckling, while the second term is proportional to the twist per unit length due to St. Venant's torsion—a term which is constant across the section. These are multiplied by appropriate coefficients to be consistent with the corresponding component of the stress vector.

Stress–strain relations

To match the strain vector $\{\varepsilon\}$ defined in eqn (9), a stress vector $\{\sigma\}$ is defined in the following manner:

$$\{\sigma\} = \{N_x \quad N_y \quad N_{xy} \quad M_x \quad M_y \quad M_{xy}\} \tag{9}$$

where N_x and N_y are the normal stress resultants in the longitudinal and transverse directions, respectively, and N_{xy} is the in-plane shearing stress resultant; M_x and M_y are the bending moments in the x–z and y–z planes, respectively, and M_{xy} is the twisting moment. All these quantities are defined over a unit length of the plate middle surface. The constitutive relationship for the linearly elastic and isotropic material may then be stated in the form

$$\{\sigma\} = [D]\{\varepsilon\} \tag{10}$$

where $[D]$ takes the form

$$[D] = \frac{Et}{(1-\nu^2)} \left[\begin{array}{ccc|ccc} 1 & \nu & 0 & & & \\ \nu & 1 & 0 & & 0 & \\ 0 & 0 & \dfrac{(1-\nu)}{2} & & & \\ \hline & & & \dfrac{t^2}{12} & \dfrac{\nu t^2}{12} & 0 \\ & 0 & & \dfrac{\nu t^2}{12} & \dfrac{t^2}{12} & 0 \\ & & & & & \dfrac{(1-\nu)t^2}{24} \end{array}\right] \tag{11}$$

and E and ν are Young's modulus and Poisson's ratio, respectively, and t is the thickness of the plate element.

Finite element discretization

The overall quantities (U, V, W, θ) are discretized in the longitudinal direction using the finite element method as follows:

$$\begin{Bmatrix} U \\ V \\ W \\ \theta \end{Bmatrix} = \begin{Bmatrix} U_i \\ V_i \\ W_i \\ \phi_i \end{Bmatrix} \phi_i(\xi) \quad (i = 1, \ldots, 4) \tag{12}$$

where $U_i, \ldots, \beta_i$ are the degrees of freedom and ϕ_i the cubic polynomials defined over the interval $(-1, 1)$ and given by

$$\begin{aligned} \phi_1 &= \tfrac{1}{4}(2 - 3\bar{x} + \bar{x}^3); \quad \phi_2 = \tfrac{1}{4}(1 - \bar{x} - \bar{x}^2 + \bar{x}\bar{\xi}^3) \\ \phi_3 &= \tfrac{1}{4}(2 + 3\bar{x} - \bar{x}^3); \quad \phi_4 = \tfrac{1}{4}(-1 - \bar{x} + \bar{x}^2 + \bar{x}^3) \end{aligned} \tag{13a-d}$$

with $\bar{x} = 2x/L_e$, L_e being the length of the element. The modulation of the local buckling amplitudes is described by setting

$$\xi_i = \xi_{ij} f_j(\bar{x}) \quad (j = 1, 2; i = 1, 3) \tag{14}$$

where ξ_{ij} is the amplitude of the ith mode at the jth node and f_j are linear functions given by

$$f_1 = \left(\frac{1-\bar{x}}{2}\right); \quad f_2 = \left(\frac{1+\bar{x}}{2}\right). \tag{15a, b}$$

In computation, functions f_i are treated as slowly varying in the sense of [1, 2] and drastic simplification is achieved thereby. The 16 degrees of freedom in eqn (12) together with the six local buckling degrees of freedom in eqn (14) describe, in the most general case, the behavior of an element of a thin-walled member.

Computation of stiffness matrices

The equations of equilibrium of the structure are written using the principle of virtual work in the notation in Ref. [12]. Let $\{a\}$ be the vector of the nodal degrees of freedom of the structure. Then

$$\int_v \{\sigma\}^T \{d\varepsilon\}\, dV - \{da\}^T \{P_e\} = 0 \tag{16}$$

where the integration is over the entire volume of the (undeformed) structure. The linearized strain increment $\{d\varepsilon\}$ is expressed in terms of the virtual displacements given by $\{da\}$ as follows:

$$\{d\varepsilon\} = [B]\{da\} \tag{17}$$

where matrix $[B]$ is a function of the current displacements. The equations of equilibrium may then be expressed in the form

$$\{F\} = \int_v [B]^T \{\sigma\}\, dv - \{P_e\} = 0. \tag{18}$$

The use of a Newton–Raphson procedure for solution of incremental degreees of freedom in a load step, would first involve the establishment of a relation between $\{da\}$ and $\{dF\}$. Taking variations of eqn (18) with respect to $\{da\}$ and using eqns (10) and (17), we have

$$\{dF\} = [[K_L] + [K_\sigma]]\{da\} = [K_T]\{da\} \tag{19}$$

where $[K_T]$ is the tangential stiffness matrix

$$[K_L] = \int_v [B]^T [D][B]\, dv \tag{20}$$

which consists of terms arising out of the linear part of the strain–displacement relations including the influence of the current geometry; $[K_\sigma]$ is the initial stress matrix given by

$$[K_\sigma]\{da\} = \int_v d[B]^T [D]\{\varepsilon\}\, dv. \tag{21}$$

Replacing $\{dF\}$ by the load increment in the first instance and subsequently by the unbalanced nodal forces computed using eqn (18) the incremental degrees of freedom are solved for iteratively.

In the present problem, considerable computational simplicity is achieved by the orthogonality of the trigonometric functions characterizing the local buckling deformation and treating ϕ_i and f_i as slowly varying functions. In effect, these functions are approximated to be piecewise constants over a wavelength of local buckling. As a step in this process of simplification, $[B]$ and $\{\varepsilon\}$ are written in the form

$$[B] = [B_0] + \sum_{n=1}^{2} [B_n^c] \cos(nm\pi x/L) + [B_n^s] \sin(nm\pi x/L) \tag{22a}$$

$$\{\varepsilon\} = \{\varepsilon_0\} + \sum_{n=1}^{2} \{\varepsilon_n^c\} \cos(nm\pi x/L) + \{\varepsilon_n^s\} \sin(nm\pi x/L) \tag{22b}$$

where the matrices and vectors on the right-hand side are free of trigonometric terms. Using

eqns (22a) and (22b) and the concept of slowly varying functions as applied to f and ϕ, the $[K_L]$ and $[K_\sigma]$ matrices can be expressed in the compact form as

$$[K_L] = \int_v \left\{ [B_0]^T [D] [B_0] + \frac{1}{2} \sum_{n=1}^{2} [[B_n^c]^T [D] [B_n^c] + [B_n^s]^T [D] [B_n^s]] \right\} dv \tag{23a}$$

$$[K_\sigma] \{da\} = \int_v \left\{ d[B_0]^T [D] \{\varepsilon_0\} + \frac{1}{2} \sum_{n=1}^{2} [d[B_n^c]^T [D] \{\varepsilon_n^c\} + d[B_n^s]^T [D] \{\varepsilon_n^s\}] \right\} dv \tag{23b}$$

and the vector of internal resisting forces takes the form

$$\{P_i\} = \int_v \left\{ [B_0]^T [D] \{\varepsilon_0\} + \frac{1}{2} \sum_{n=1}^{2} [[B_n^c]^T [D] \{\varepsilon_n^c\} + [B_n^s]^T [D] \{\varepsilon_n^s\}] \right\} dv. \tag{24}$$

It is important to note that for the strain–displacement relations of the present problem (eqn (9)), all the terms which give rise to the interaction are contained in the matrix $[B_0]$; the remaining $[B]$ matrices contain local buckling terms only and thus the integrations involving them in eqns (23) and (24) give rise only to a 6×6 sub-matrix of $[K_T]$ and 6×1 sub-vector of $\{P_i\}$ for each element. These are computed in terms of the current values of ξ_{ij} using exact integration.

The contribution to the element stiffness matrix arising from $[B_0]$ takes the form

$$[k] = \begin{bmatrix} k^{00} & k^{0l} \\ k^{l0} & k^{ll} \end{bmatrix}. \tag{25}$$

Of these the terms in the k^{00} matrix result from integrations of products of derivatives of ϕ functions which are independent of y and are computed using either exact or Gaussian integration.

The terms in the k^{l0} matrix arise from products of:

(i) the local buckling quantities, variable with respect to y and those associated with trigonometric terms ($n = 0, 1, 2$, eqns (22)) and the modulating functions f, and

(ii) the overall buckling quantities, which are functions of ϕ and their derivatives.

Considerable simplification in integration is achieved here by the use of the concept of "slowly varying" functions for f and ϕ. The fourth-order Gaussian quadrature is employed across each strip and along the length of the element in evaluating these terms. The k^{ll} matrix arises exclusively from local buckling functions and is derived by exact integration as before. A similar strategy is used in setting up of the load vector $\{P_i\}$ (eqn (24)).

Solution process

The solution process is initiated with the values of initial imperfections as the starting displacements of the structure at the zero level of stresses. The displacements and stresses are accumulated as the solution proceeds along the equilibrium path. An automatic load incrementation scheme[13] is employed to negotiate the limit point of the load–deflection path.

EXAMPLES

The theory outlined in the previous section was implemented through a computer program. The theory and the computer program were checked for internal consistency, agreement with some well-established results and convergence of the results with increasing degrees of freedom. These results are presented elsewhere[14]. In this section a few examples illustrative of the behavior of compression members having a single axis of symmetry are presented. The results are compared wherever possible with those available in the literature.

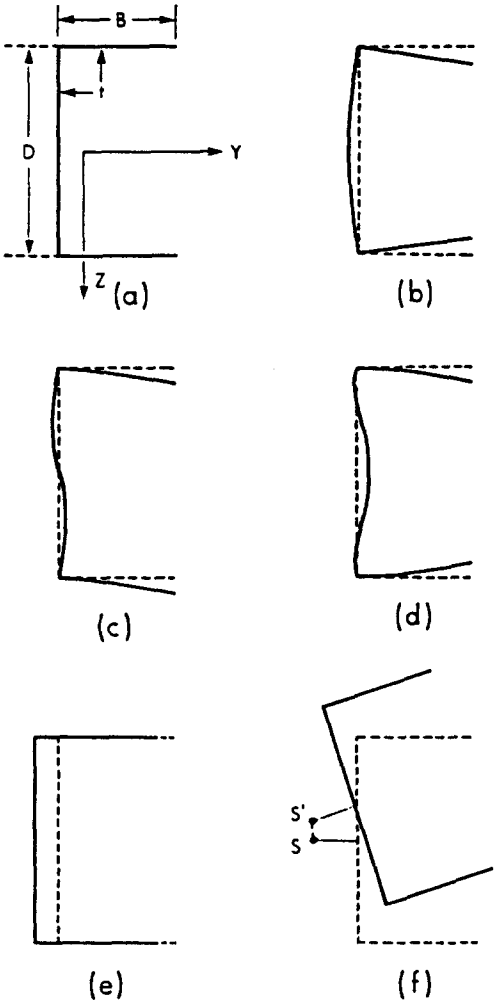

Fig. 3. (a) Cross-section of the columns investigated. (b) - (d) The primary (ξ_1) and the two secondary local modes (ξ_2, ξ_3), respectively. (e), (f) The Euler and the flexural torsional modes of buckling.

The columns are considered simply supported and are modelled by 24 longitudinal strips in the local buckling analysis and five elements over half the column for the interactive buckling analysis. Poisson's ratio is assumed to be 0.3 in all the calculations.

Channel-section columns

A column with a single axis of symmetry (Fig. 3(a)) may lose its stability by either flexural buckling (bending in the plane of symmetry) or flexural–torsional buckling. The cross-sectional displacements associated with these modes are illustrated in Figs 3(e) and (f), respectively. In the absence of local buckling the mode corresponding to the lower of the two critical stresses governs the behavior of the column; in the presence of local buckling, there exists a possibility of interaction of the two overall modes. The local modes of buckling that are relevant for the channel-section column are illustrated in Figs 3(b)–(d). Of these mode (1) (Fig. 3(b)) is the primary one as it corresponds to the lowest local critical stress and dictates the wavelength of modes (2) and (3) triggered respectively by bending of the column in the Z–X (perpendicular to the plane of symmetry) and Y–X (in the plane of symmetry) planes, respectively. These have the same wavelength as mode (1).

Two channel-section columns designated by C-1 and C-2, respectively, are considered. For section C-1, the flexural mode is the critical one while for section C-2, the flexural–torsional mode is critical. The properties of the section and all the five relevant critical stresses are given in Table 1 in their dimensionless forms, namely σ_1/E, σ_2/E, σ_3/E, σ_v/E, and σ_{w0}/E. Note that σ_1, σ_2 and σ_3 are the three local critical stresses corresponding to the

Table 1. Properties of the channel-section columns

Section type	Geometric proportions Flange D/t	Web B/t	Length L/t	m	Local critical stresses $\sigma_1 E\times10^3$	$\sigma_2 E\times10^3$	$\sigma_3/E\times10^3$	Overall critical stresses $\sigma_c E\times10^3$	$\sigma_{cw}/E\times10^3$
C-1	75	25	900	11	0.676	1.44	2.17	0.711	0.769
C-2									
Cases (i)–(iii)	50	25	650	11	1.05	1.44	3.31	1.52	1.05
Case (iv)	50	25	390	6	1.05	1.44	3.31	4.22	2.63

modes illustrated in Figs 3(b)–(d), respectively, and σ_c and σ_{cw} are respectively the flexural and flexural–torsional critical stresses. The behavior of the column is *not* symmetric for flexural buckling and would be governed by the sense of the initial imperfection $\bar{V}$[5, 15]. In the following examples, $\bar{V}$ is assumed in the adverse sense, i.e. the one that would cause additional compression on the slender outstands (webs) as the column bends.

The column with section C-1

From Table 1, it is seen that for this column the primary local critical stress and the flexural critical stress are very close to each other ($\sigma_c/\sigma_1 = 1.052$); however, the flexural–torsional critical stress is also in close vicinity ($\sigma_{cw}/\sigma_1 = 1.138$). Thus even though interaction of the primary local and flexural buckling is expected to be the dominant feature of the response, the influence of the flexural–torsional buckling cannot be discounted.

Case (i). In this example, all the degrees of freedom corresponding to the flexural–torsional mode of buckling are eliminated from the analysis, i.e. $W = \theta = 0$. (This can be done in the same manner as applying boundary conditions.) The initial imperfection in the local mode ($\bar{\xi}_1$) is given by the maximum cross-sectional displacement divided by t and is taken as 0.05. The overall imperfection is given by the initial central deflection and is taken as $\bar{V} = L/2250t$. The results of the analysis are shown in Fig. 4 where they are also compared with those of Benito and Sridharan[5]. In Fig. 4, the non-dimensional load is plotted against non-dimensional mid-span deflections ξ_1, ξ_2, and V/t. Benito and Sridharan employed a two-degrees-of-freedom model to study the two-mode interaction problem. In addition, they considered a mixed second-order displacement field that corresponded closely with mode (3) (Fig. 3(d)) of the present analysis. The two analyses have many similarities, but the present analysis incorporates the ξ_3 mode as a participating mode (which is thus treated more accurately) and allows the amplitudes ξ_1 and ξ_3 to modulate along the length of the column. However, the two analyses produce results which are in good agreement with each other. The present analysis gives a slightly lower maximum load of $\sigma_u/\sigma_1 = 0.846$ compared to 0.882 of Benito and Sridharan.

Case (ii). As was noted earlier, the two overall critical stresses are close to each other (cf. $\sigma_{cw}/\sigma_1 = 1.138$ with $\sigma_c/\sigma_1 = 1.052$). Therefore, there exists a possibility of an active participation of the flexural–torsional mode in the process of interaction. In order to investigate this phenomenon, the same problem is analyzed with the following magnitudes

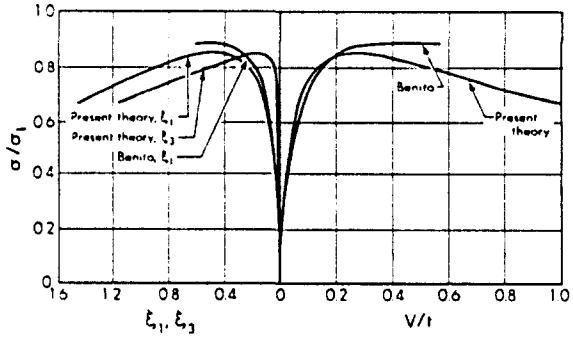

Fig. 4. The load–deflection characteristics of channel-section column C-1 (Table 1): $W = \theta = 0$, $\bar{\xi}_1 = 0.05$, $\bar{V} = L/2250$.

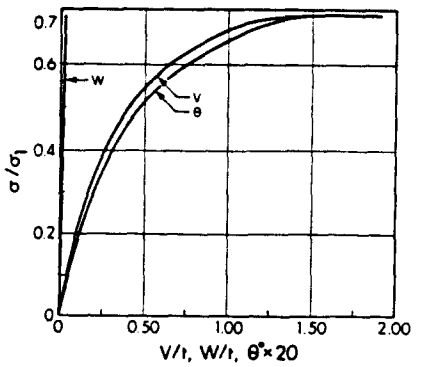

Fig. 5(a). The overall load-deflection characteristics of channel-section column C-1 (Table 1): $\xi_1 = 0.05$, $\bar{V} = L/2250$, $\bar{W} = L/2250$, $\bar{\theta} = 1$.

of initial imperfections: $\xi_1 = 0.1$, $\bar{V} = L/2250t$, $\bar{W} = L/2250t$ and $\theta = 1°$. The maximum load as given by σ_u/σ_1 in this case is found to be 0.719—a value which is 15% lower than that obtained in case (i). The load–deflection characteristics of this problem are shown in Figs 5(a) and (b). Figure 5(a) plots the dimensionless load σ/σ_1 against the maximum values of the overall displacements. It is interesting to note that the flexural deflection W, associated with the flexural–torsional (W–θ) mode does grow but at an extremely slow rate in spite of the presence of a significant magnitude of initial imperfection $\bar{W}$ associated with it. This is due to the high flexural rigidity of the section for bending in the W-direction as is evidenced by the dominance of the torsional component over the flexural component of the deformation in the buckling mode where $W : y_0\theta = 1.0 : 12.36$. Further, the resistance to twisting decreases as the outstands lose some of their effective stiffness as a result of local buckling. As a consequence the angle of twist is seen to grow considerably, but W remains inactive.

The plots of the non-dimensional load vs the maximum amplitudes (at $x = L/2$) of the three local modes are shown in Fig. 5(b). The displacements in the primary local mode (ξ_1) start developing from the outset of the loading history. Both the warping resistance of the section to torsion and the bending in the Z-direction (the latter, a comparatively minor effect) induce compression on one side and tension on the other side of the line of symmetry. As a direct result, the displacements in the form of the secondary local mode (ξ_2) are seen to grow rapidly. The displacements in the form of mode (3) are slow to develop in the earlier stages of the loading history because of the high value of σ_3/σ_1, but as the column approaches its peak load ξ_3 takes on values which are not small in comparison to ξ_1 and ξ_2.

Figure 5(b) also shows the variation of the local buckling amplitudes at the peak load. Although the amplitude ξ_1 changes very little for this simply supported column problem, the amplitudes for the secondary local modes are seen to modulate considerably.

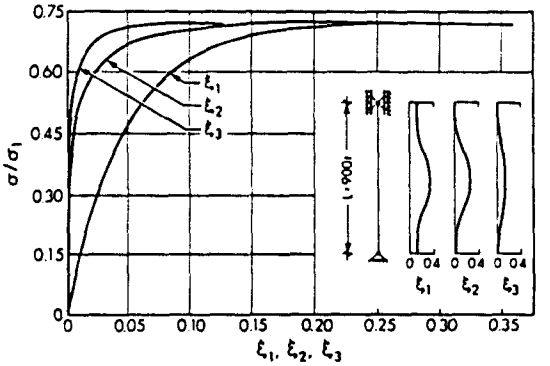

Fig. 5(b). The local load–deflection characteristics of channel-section column C-1 (Table 1): $\xi_1 = 0.05$, $\bar{V} = L/2250$, $\bar{W} = L/2250$, $\bar{\theta} = 1$.

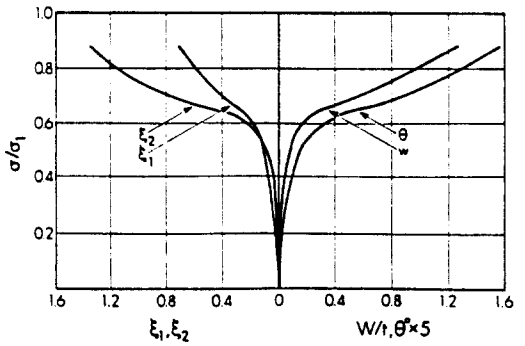

Fig. 6. The local and flexural–torsional load–deflection characteristics of channel-section column C-2 (Table 1): $\bar{\xi}_1 = 0.1$, $\bar{W} = 0$, $\bar{\theta} = L/2200y_0$, $\bar{V} = 0$, $L = 650t$.

The results of this example problem confirm the general view that the interaction of local and overall buckling results in severe imperfection sensitivity for near-coincident buckling. It also indicates that the flexural–torsional mode can play a significant role in the interaction even though $\sigma_{w\theta} > \sigma_{t\cdot}$.

The column with section C-2

The section of this column has a relatively narrow flange compared to section C-1 (Table 1) and as a result the flexural–torsional mode governs the initial buckling behavior. The reduced slenderness of the flange also has the effect of increasing σ_1 and bringing it closer to σ_2 and σ_3—these values being now governed by the slenderness of the outstands. The behavior of the column is studied varying the levels of the initial imperfections in cases (i)–(iii) below. In case (iv), the length of the column is reduced thus separating the magnitudes of the governing local and overall critical stresses by a wide margin.

Case (i). The interaction of the local and flexural–torsional buckling is examined by excluding the flexural buckling mode from the analysis. The initial imperfections are: $\bar{\xi}_1 = 0.1$; $\bar{W} = 0.0$, and $\bar{\theta} = (L/2200)/y_0$. The results of this analysis are shown in Fig. 6 where the non-dimensional load is plotted against maxima of W/t, θ, ξ_1 and ξ_2. The column is not seen to be imperfection sensitive for the type of interaction considered. It is seen (Fig. 6) that at about $\sigma/\sigma_1 = 0.6$ the column starts developing huge deformations with a corresponding drop in the rate of increase the axial load carried. The column becomes somewhat stiffer around $\sigma/\sigma_1 = 0.68$ and then continues indefinitely to carry additional load. This behavior is similar to that observed by Benito[15]. (Such a behavior will not be observable in practice because of the reality of flexural buckling excluded from the analysis.)

Case (ii). The flexural–torsional mode of buckling is suppressed in this example and the interaction between the overall flexural buckling and local buckling is studied in isolation. The assumed initial imperfections are: $\bar{\xi}_1 = 0.1$ and $\bar{V} = L/1000$. In Fig. 7, σ/σ_1 is plotted against maxima of V/t and ξ_1 and ξ_3, respectively. The maximum load as given by σ_u/σ_1 is found to be 0.624. Hence the column is imperfection sensitive though σ_t is about

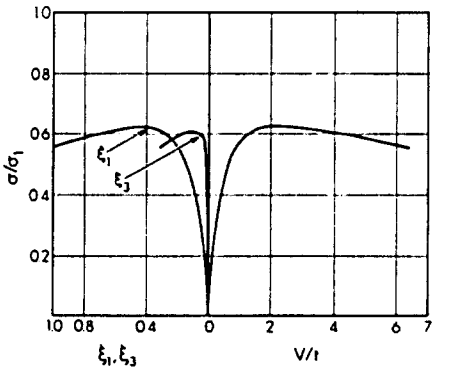

Fig. 7. The local and flexural load–deflection characteristics of channel-section column C-2 (Table 1): $\bar{\xi}_1 = 0.1$, $\bar{V} = L/1000$, $\bar{W} = \bar{\theta} = 0$, $L = 650t$.

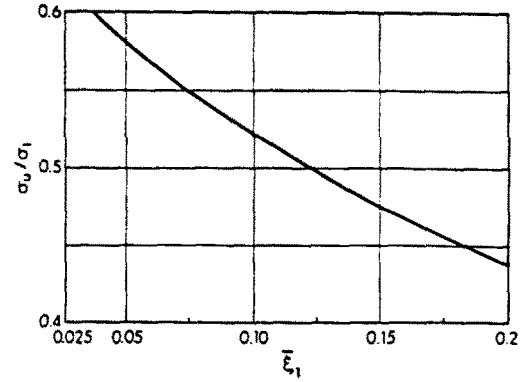

Fig. 8. Local imperfection sensitivity of channel-section column C-2 (Table 1): $\bar{V} = L/2000$, $\bar{W} = L/10{,}000$, $\bar{\theta} = 1^\circ$, $L = 650t$.

45% higher than σ_1—an observation which agrees with the general finding of Ref. [15]. It follows that the essence of the interaction lies in the flexural mode rather than in the flexural–torsional mode.

Case (iii). The simultaneous interaction of local, flexural and flexural–torsional buckling modes is investigated in this example. The assumed overall initial imperfections are: $\bar{V} = L/2000$, $\bar{W} = L/10{,}000$ and $\bar{\theta} = 1^\circ$. The local imperfection is assumed in the primary mode only and this is varied from $\bar{\xi}_1 = 0$ to 0.2. Figure 8 shows the variation of the maximum non-dimensional load with $\bar{\xi}_1$ with the other imperfection magnitudes kept constant. It is found that the column is significantly imperfection sensitive. The load–deflection characteristics for a case with $\bar{\xi}_1 = 0.1$ are shown in Fig. 9. From a comparison with case (ii), it is seen that the maximum load is reduced significantly in this case (cf. $\sigma_u/\sigma_1 = 0.52$ vs 0.63) despite the fact that the overall imperfection in this case has been reduced by half. This once again underlines the significant role of the flexural–torsional mode when it acts in conjunction with the purely flexural mode. The extent of participation of the various local and overall modes is clearly seen in Fig. 11. In particular, the secondary local mode associated with the flexural–torsional buckling is seen to play an important role. It appears, however, that none of the five modes can be neglected in an accurate description of the behavior and determination of the maximum load of the column.

Case (iv). In this case the length of the column is reduced to 0.6 of its length in the previous cases so that $L = 390t$ and $m = 6$. The values of the overall critical stresses are now well separated from the primary local critical stress ($\sigma_{w0}/\sigma_1 = 2.50$ and $\sigma_{t}/\sigma_1 = 4.02$). Imperfections are assumed in the same manner as in case (iii), i.e. $\bar{\xi}_1 = 0.1$, $\bar{V} = L/2000$, $\bar{W} = L/10{,}000$ and $\bar{\theta} = 1^\circ$. The load–deflection characteristics are shown in Fig. 10. The behavior is similar to that observed in case (iii). The maximum load attained in this case as given by σ_u/σ_1 is only 0.75 (which in the absence of imperfections cannot be smaller than 1.0). Thus the fact that the overall critical stresses are considerably higher in this case changed neither the severe imperfection sensitivity nor the general behavior of the column.

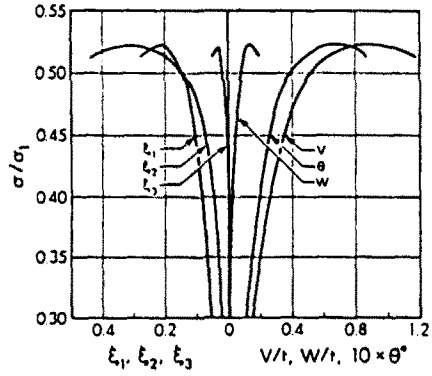

Fig. 9. The load–deflection characteristics of channel-section column C-2 (Table 1): $\bar{\xi}_1 = 0.1$, $\bar{V} = L/2000$, $\bar{W} = L/10{,}000$, $\bar{\theta} = 1^\circ$, $L = 650t$.

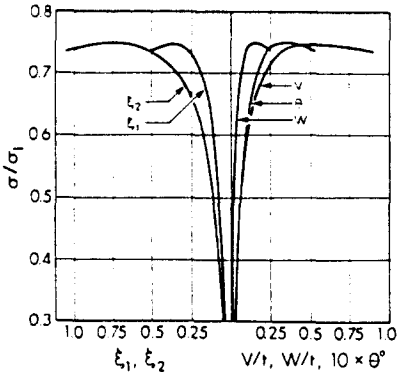

Fig. 10. The load-deflection characteristics of channel-section column C-2 (Table 1): $\bar{\xi}_1 = 0.1$, $\bar{V} = L/2000$, $\bar{W} = L/10{,}000$, $\bar{\theta} = 1$, $L = 390t$.

Stiffened panel

Interactive buckling and imperfection sensitivity of the Tvergaard panel[1–3, 16] are studied in this section. The cross-sectional details of the panel are shown in Fig. 11. The panel has a very slender plate stiffened by stocky ($t_s/t \simeq 4.5$) stiffeners. Because the panel is a part of an "infinitely" wide plate, the flexural-torsional mode of buckling does not exist for the panel. The panel is simply supported over a span of $4B$. B being the width of the panel. The primary local mode consists of six half-waves ($m = 6$) each of length $2B/3$. The initial buckling analysis of the panel with $m = 6$ and the mixed second-order field arising by the interaction of the primary local and the overall mode indicated[15] that there is no relevant secondary local mode which could be triggered by interaction. Thus the major interaction takes place between the Euler-type overall mode and a single amplitude-modulated local mode. This is a case of near-coincident buckling with $\sigma_1 = 0.475 \times 10^{-3}$ and $\sigma_v/\sigma_1 = 1.036$. [Note that the present analysis does not consider shear-lag effects for overall buckling and the probable error introduced due to this assumption in this case ($L/B = 4$) has been discussed by Koiter and Pignataro[2].]

The load deflection characteristics are shown in Fig. 12 in which the non-dimensional displacement quantities ξ_1 and V/t at mid-span are plotted against the non-dimensional load σ_u/σ_1. Three cases are illustrated: case (i) $\bar{V} = 0.0$; case (ii) $\bar{V} = L/4000$; and case (iii) $\bar{V} = L/2000$. The local imperfection $\bar{\xi}_1$ is assumed to be 0.05 for all three cases. Though the panel has near-coincident critical stresses, it is not very imperfection sensitive. The maximum load is almost the same for all three cases considered. For cases (ii) and (iii), the behavior of the column resembles that of a solid Euler column with a reduced stiffness; the deflections increase without limit as the column approaches asymptotically the "buckling" load the value of which is not governed by the imperfection magnitudes. Figure 12 also shows the variation of the function modulating the local buckling amplitude for case (ii) at $\sigma_u/\sigma_1 = 0.882$. The amplitude is seen to vary rather significantly showing thus the importance of the phenomenon of amplitude modulation in the interactive buckling problems.

The panel problem discussed here has been studied by Tvergaard[3, 16] and Koiter and Pignataro[1, 2]. The present analysis is similar to that of Ref. [1]. The principal difference is that the latter uses a "lower bound approach" for the post-local-buckling analysis.

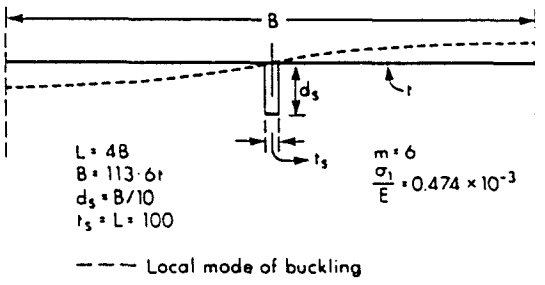

Fig. 11. Details of the Tvergaard panel.

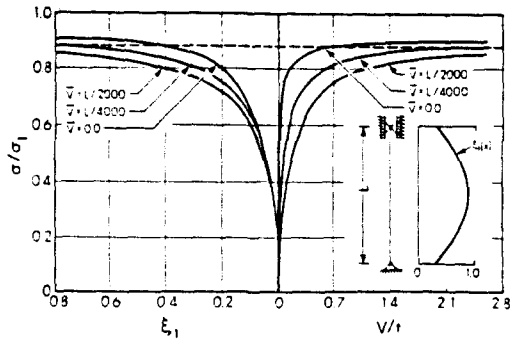

Fig. 12. The load deflection characteristics of the Tvergaard panel ($\bar{\xi}_1 = 0.05$).

Furthermore, the present analysis employs a vastly larger number of degrees of freedom; and for a column with no overall imperfections, it accounts for the interaction between local buckling and overall bending from the very outset of the loading history. For the case with $V = 0$, Ref. [1] indicates that the maximum load as given by σ_u/σ_1 has a lower bound of 0.889 (however large the value of $\bar{\xi}_1$ may be). This load level is indicated in Fig. 12 by a dashed line parallel to the V-axis. Again for $V = 0$ and $\bar{\xi}_1 = 0.05$, Ref. [2] reports a value of $\sigma_u/\sigma_1 = 0.922$. In this case, the present analysis yields a central deflection of $L/124$ for a value of $\sigma/\sigma_1 = 0.912$ (not shown). Beyond this point, the non-dimensional load continues to increase, though extremely slowly, with an enormous increase in the deflections. Despite the differences, both the analyses are seen to be in very good agreement indeed.

CONCLUSIONS

A new versatile analytical model for interactive buckling in thin-walled columns has been presented. The following are some of the important features of the new model.

(i) It can deal with the problem of simultaneous interaction of overall bending in two principal directions and twisting of the column with local buckling.

(ii) The local buckling deformation contributed by a primary local mode and two relevant secondary local modes together with all the six associated second-order displacement fields are duly taken into account. These fields are computed using the finite strip method.

(iii) The overall displacements and the modulation of the amplitudes of the local buckling modes are modelled using a one-dimensional finite element formulation.

(iv) As a result of (i) (iii), the model is applicable in the analysis of columns and beam-columns of arbitrary cross-section and end conditions.

Some examples of compression members having a single axis of symmetry are presented in this paper. The interaction of the local, flexural and flexural-torsional modes of buckling with local buckling in channel-section columns is found to be very imperfection sensitive. The load deflection curves show well-defined limit points even for the case of well-separated critical stresses. Though the flexural buckling and the primary local modes are the essential components in the interaction, the inclusion of the flexural torsional mode and associated secondary mode is necessary for a reliable prediction of the capacity of the columns.

The severe imperfection sensitivity of the channel-section columns noted here is in marked contrast with the behavior of the columns with doubly symmetric sections which for values of σ_0/σ_1 of 2.0 or above, often exhibit little or no sensitivity to imperfections and behave like solid Euler columns with a reduced stiffness.

However, it is not possible to make a generalization of the behavior of columns with a single axis of symmetry based on the example of channel-section columns. The Tvergaard panel is a case in point. It is a case of near-coincident buckling but exhibits only a moderate level of imperfection sensitivity and for larger magnitudes of initial imperfection, the solid Euler column behavior cited earlier.

Acknowledgement—The work reported in this paper was funded from a grant from NSF (Grant No. 8318423). However, any opinions expressed herein are solely the responsibility of the authors and do not necessarily reflect those of the NSF.

REFERENCES

1. W. T. Koiter and M. Pignataro, *An Alternative Approach to the Interaction between Local and Overall Buckling in Stiffened Panels*, IUTAM Symposium, Cambridge, Massachusetts, 1974, *Buckling of Structures* (Edited by B. Budiansky), pp. 133–148. Springer, Berlin (1976).
2. W. T. Koiter and M. Pignataro, A general theory for the interaction between local and overall buckling in stiffened panels. Delft University of Technology, Department of Mechanical Engineering, Report WTHD-83 (1976).
3. V. Tvergaard, Imperfection sensitivity of a wide integrally stiffened panel under compresssion. *Int. J. Solids Structures* **9**, 177–192 (1973).
4. A. von der Neut, *Mode Interaction in Stiffened Panels*, IUTAM Symposium, Cambridge, Massachusetts, 1974, *Buckling of Structures* (Edited by B. Budiansky), pp. 117–132. Springer, Berlin (1976).
5. R. Benito and S. Sridharan, Interactive buckling with finite strips. *Int. J. Numer. Meth. Engng* **21**, 145–161 (1985).
6. S. Sridharan and M. A. Ali, An improved interactive buckling analysis of thin-walled columns having doubly symmetric sections. *Int. J. Solids Structures* **22**, 428–443 (1986).
7. S. Sridharan and M. A. Ali, Interactive buckling in thin-walled beam columns. *J. Engng Mech. ASCE* **111**(12), 1470–1486 (1985).
8. S. Sridharan and T. R. Graves-Smith, Postbuckling analyses with finite strips. *J. Engng Mech. Div. ASCE* **EM5**, 869–888 (1981).
9. T. R. Graves-Smith and S. Sridharan, A finite strip method for the post-locally buckled analysis of plate structures. *Int. J. Mech. Sci.* **20**, 833–842 (1978).
10. S. Sridharan, A finite strip analysis of locally buckled plate structures subject to nonuniform compression. *Engng Struct.* **4**, 249–255 (1982).
11. T. V. Galambos, *Structural Members and Frames*. Prentice-Hall, Englewood Cliffs, New Jersey (1968).
12. O. C. Zienkiewicz, *The Finite Element Method*. McGraw-Hill, London (1977).
13. G. Powell and J. Simons, Improved iteration strategy for nonlinear structures. *Int. J. Numer. Meth. Engng* **17**, 1455–1467 (1981).
14. M. A. Ali, A new model for elastic interactive buckling. Thesis submitted in partial fulfillment of the requirements of the D.Sc. Degree, Washington University, St. Louis (December 1986).
15. R. Benito, Static and dynamic interactive buckling analysis of plate assemblies. Thesis submitted in partial fulfillment of the requirements of the D.Sc. Degree, Washington University, St. Louis (May 1983).
16. V. Tvergaard, Influence of postbuckling behavior on optimum design of stiffened panels. *Int. J. Solids Structures* **9**, 1519–1534 (1973).